

Conserved Residues and Their Role in the Structure, Function, and Stability of Acyl-Coenzyme A Binding Protein[†]

Birthe B. Kragelund,[‡] Keld Poulsen,[§] Kim Vilbourn Andersen,^{‡,||} Trausti Baldursson,[‡] Jenny B. Krøll,[‡] Thomas B. Neergård,[§] Jan Jepsen,[§] Peter Roepstorff,[‡] Karsten Kristiansen,[‡] Flemming M. Poulsen,^{*,‡} and Jens Knudsen^{*,§}

Department of Chemistry, Carlsberg Laboratory, Gl. Carlsberg Vej 10, DK-2500 Valby, Copenhagen, Denmark, Institute of Biochemistry, Odense University, Campusvej 55, DK-5230 Odense M, Denmark, and Department of Molecular Biology, Odense University, Campusvej 55, DK-5230 Odense M, Denmark

Received October 13, 1998; Revised Manuscript Received December 16, 1998

ABSTRACT: In the family of acyl-coenzyme A binding proteins, a subset of 26 sequence sites are identical in all eukaryotes and conserved throughout evolution of the eukaryotic kingdoms. In the context of the bovine protein, the importance of these 26 sequence positions for structure, function, stability, and folding has been analyzed using single-site mutations. A total of 28 mutant proteins were analyzed which covered 17 conserved sequence positions and three nonconserved positions. As a first step, the influence of the mutations on the protein folding reaction has been probed, revealing a folding nucleus of eight hydrophobic residues formed between the N- and C-terminal helices [Kragelund, B. B., et al. (1999) *Nat. Struct. Biol.* (In press)]. To fully analyze the role of the conserved residues, the function and the stability have been measured for the same set of mutant proteins. Effects on function were measured by the extent of binding of the ligand dodecanoyl-CoA using isothermal titration calorimetry, and effects on protein stability were measured with chemical denaturation followed by intrinsic tryptophan and tyrosine fluorescence. The sequence sites that have been conserved for direct functional purposes have been identified. These are Phe5, Tyr28, Tyr31, Lys32, Lys54, and Tyr73. Binding site residues are mainly polar or charged residues, and together, four of these contribute approximately 8 kcal mol⁻¹ of the total free energy of binding of 11 kcal mol⁻¹. The sequence sites conserved for stability of the structure have likewise been identified and are Phe5, Ala9, Val12, Leu15, Leu25, Tyr28, Lys32, Gln33, Tyr73, Val77, and Leu80. Essentially, all of the conserved residues that maintain the stability are hydrophobic residues at the interface of the helices. Only one conserved polar residue, Gln33, is involved in stability. The results indicate that conservation of residues in homologous proteins may result from a summed optimization of an effective folding reaction, a stable native protein, and a fully active binding site. This is important in protein design strategies, where optimization of one of these parameters, typically function or stability, may influence any of the others markedly.

The acyl-coenzyme A binding proteins (ACBPs)¹ are highly conserved proteins of typically 86 residues, which are suggested to play an important role in intracellular acyl-CoA transport and metabolism (1). ACBP has proven to be an excellent model system for studies of both protein dynamics (2, 3) and completely reversible protein folding (4–6). The fully reversible folding processes of the bovine, rat, and yeast proteins have all been shown to occur in

apparent two-state reactions without any observable intermediate states (5).

Recently, the primary sequences of 24 eukaryote ACBP sequences were compared, including those from species from both fungi/plant and animal kingdoms. This comparison showed that 26 positions encompassing both polar and nonpolar amino acid types have been conserved throughout

[†] This paper is a contribution from the Danish Protein Engineering Research Centre, which is supported jointly by the Agricultural, Health, Natural, and Technical Science Research Councils of Denmark. The work was supported partly by the CISFEM biotechnology center.

* To whom correspondence should be addressed. F.M.P.: e-mail, fmp@crc.dk; telephone, +45 33 27 53 48; fax, +45 33 27 47 08. J.K.: e-mail, jkk@biochem.ou.dk; telephone, +45 65 57 24 67; fax, +45 65 57 24 57.

[‡] Carlsberg Laboratory.

[§] Institute of Biochemistry, Odense University.

^{||} Present address: Enzyme Design, Novo-Nordisk A/S, Novo Allé, DK-2880 Bagsværd, Denmark.

¹ Department of Molecular Biology, Odense University.

¹ Abbreviations: ACBP, acyl-coenzyme A binding protein; CoA, coenzyme A; GuHCl, guanidinium chloride; ITC, isothermal titration calorimetry; NMR, nuclear magnetic resonance; F5A, bovine ACBP mutant containing the Phe5 → Ala substitution; A9G, Ala9 → Gly; V12A, Val12 → Ala; L15A, Leu15 → Ala; P19A, Pro19 → Ala; D21A, Asp21 → Ala; D21H, Asp21 → His; L25A, Leu25 → Ala; Y28A, Tyr28 → Ala; Y28N, Tyr28 → Asn; Y28F, Tyr28 → Phe; Y31N, Tyr31 → Asn; K32A, Lys32 → Ala; K32E, Lys32 → Glu; K32R, Lys32 → Arg; Q33A, Gln33 → Ala; A34G, Ala34 → Gly; T35A, Thr35 → Ala; P44A, Pro44 → Ala; K52M, Lys52 → Met; K54A, Lys54 → Ala; K54M, Lys54 → Met; E57A, Glu67 → Ala; Y73A, Tyr73 → Ala; Y73F, Tyr73 → Phe; V77A, Val77 → Ala; L80A, Leu80 → Ala; K52M/K54M, double mutant with Lys52 → Met and Lys54 → Met; SASA, solvent accessible surface area; vdW, van der Waals.

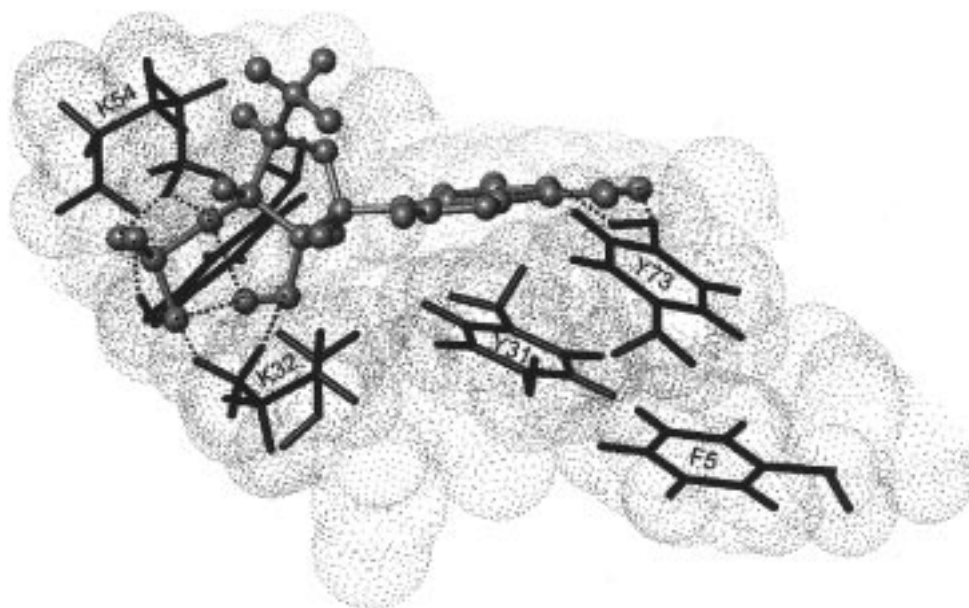


FIGURE 1: Hydrogen bonding network of ACBP and hexadecanoyl-CoA. The adenosine 3'-phosphate of the CoA head is shown as gray spheres, and the side chains of Phe5, Tyr28, Tyr31, Lys32, Lys54, and Tyr73 are shown as black sticks. Hydrogen bonds are indicated by bold dotted lines between atoms, and all atoms are also shown by their van der Waals surface.

evolution (5, 6). The role of these residues for a fast and efficient protein folding reaction was probed by mutagenesis in the bovine ACBP sequence in combination with fast-mixing spectroscopic techniques (6). The results showed that out of 18 conserved sequence sites probed seven positions were found to be important for fast folding and thus to participate in the structure formed in the rate-limiting step of the protein folding reaction (6). Additionally, a hydrophobic residue, Ile74 (homologous I/V), took part in this structure. The reversible two-state protein folding mechanism was not altered by any of the mutations introduced in the bovine variants (6).

Ligand binding to proteins is known to have a wide range of different effects on protein structure, function, and stability (7–10) and on the protein folding reaction. In ACBP, ligand binding is very tight and the preference for long chain acyl-CoA is very high (11, 12). Ligand binding does not stabilize the protein significantly against thermal denaturation (4); however, an increase in the melting temperature, T_m , measured with differential scanning calorimetry indicates that ligand binding seems to stabilize the protein significantly (B. W. Sigurskjold, personal communication). This situation is also confirmed by both amide hydrogen exchange and ^{15}N relaxation measurements (3, 4), where residues in the immediate vicinity of the ligand show decreased dynamics and thus an apparent stabilization by ligand binding. Only minor structural changes are associated with binding, and the protein topology is largely unaffected (13).

The structure of ACBP is a skew four- α -helix bundle (14, 15), and the atomic interactions between the ligand hexadecanoyl-CoA and bovine ACBP have been described in great detail with the NMR structure of the complex (13). Most of the ligand is sequestered within the protein where the ω -end (C_{16} – C_{12}) of the acyl chain is anchored in a hydrophobic cleft between helix A2 and helix A3. From here, the acyl chain bends upward around Met24 and forms a binding platform for the hydrophobic parts of the CoA head. The specificity for ligand binding resides in the ω -end of

the acyl chain together with strong electrostatic interactions with the adenosine 3'-phosphate of the CoA. In a separate study, it was shown that the 3'-phosphate is responsible for almost 40% of the total binding energy (12). This phosphate group of the ribose and the hydroxyl group are involved in an intense network of electrostatic and polar interactions where interactions with the polar parts of the side chains of Tyr28, Lys32, and Lys54 are prominent (Figure 1). The large adenine ring stacks with the aromatic ring of Tyr31, and hydrogen bonds are formed between the hydroxyl of Tyr73 and acceptors of the adenine ring itself. The interactions between the ω -end of the acyl chain and ACBP are hydrophobic and thus not as specific as the interactions found between the CoA and ACBP.

To fully analyze the role of the conserved residues in the ACBP family, a total of 28 mutant variants of bovine ACBP were constructed (Figure 2). The set of variants covers 20 sequence sites of both hydrophobic and polar/charged residues at both conserved and nonconserved positions. The method of single-site mutations has been the platform for an investigation of the contribution of each amino acid residue to ligand binding and to the stability of the native protein against chemical denaturation. It is possible that one specific residue can be evolutionally conserved for all three purposes, structure and stability, function, and efficient folding, and it may be possible from a gradual modification of that residue to establish the role of the different parts of the side chain. Two different techniques are applied. The technique of ITC is used for thermodynamic characterization of dodecanoyl-CoA binding to all variants. In the appropriate binding ranges, this technique offers the potential to directly determine the dissociation constant K_d and the molar enthalpy, $\Delta H_{\text{bind}}^\circ$, and thereby also the determination of $\Delta G_{\text{bind}}^\circ$ and $\Delta S_{\text{bind}}^\circ$ from single-titration experiments (16). The stability of the apoproteins, $\Delta G_{\text{D-N}}$, was determined from chemical denaturation by guanidinium chloride (GuHCl) of the mutant proteins using intrinsic tryptophan and tyrosine fluorescence. The obtained parameters for the apo and holo

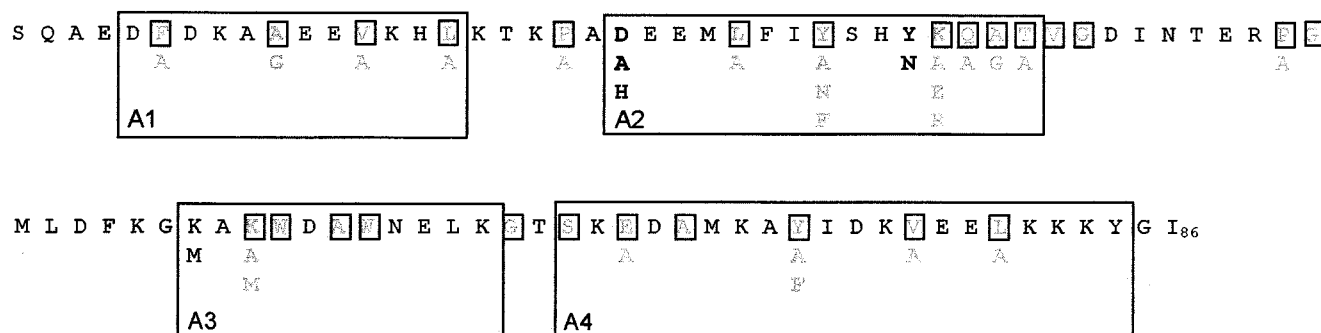


FIGURE 2: Mapping of the mutated sites to the primary sequence of bovine ACBP. The different mutations are indicated by their alternatives, and conserved residues are boxed. Residues with specific van der Waals interactions with the ligand as identified in the structure of the complex of bovine ACBP and hexadecanoyl-CoA are shown in bold, and the four α -helices are shown as boxes labeled A1–A4.

forms of bovine ACBP are analyzed and compared in relation to the position of the mutation within the structures.

EXPERIMENTAL PROCEDURES

DNA Construction. Vectors for expression of ACBP mutants were generated by site-directed mutagenesis of pKK223ACBP expressing wild type bovine ACBP (17). Two procedures were employed. Mutagenesis was carried out with mutagenic primers and standard PCR techniques using a Perkin-Elmer Cetus DNA Thermal Cycler. The wild type gene was excised from pKK223 by treatment with restriction endonucleases and replaced with the mutant gene. The new plasmids were transformed into *Escherichia coli* strain DH5 α that was used as an expression host. The constructions were verified by DNA sequencing using the model 373A DNA Sequencing System and the Taq DyeDeoxy Terminator Cycle Sequencing Kit from Applied Biosystems, Inc. The remaining mutants were generated according to the Eckstein procedure using the Amersham oligonucleotide-directed in vitro mutagenesis system following the recommendations of the manufacturer. The *EcoRI*–*HindIII* fragment of pKK223ACBP (17) was subcloned into M13mp11. Single-stranded templates were isolated according to standard procedures and used for site-directed mutagenesis using specific mutagenic oligonucleotides. Appropriate fragments harboring the desired mutations were isolated and cloned into pKK223ACBP Δ 1 for high-level expression. The sequences of all mutants were verified by the dideoxy chain termination procedure using a Pharmacia T7 DNA polymerase kit.

Expression and Purification. The proteins were expressed and purified as described previously (11, 17) with a few modifications. After homogenization in the French press, 5% (v/v) trichloroacetic acid was added, and the suspension was stirred on ice for 30 min to precipitate ACBP. The heat denaturation step was omitted. For purification on HPLC, buffer A was substituted with 96% ethanol and 0.1% trichloroethanol and buffer B with H₂O and 0.1% trichloroethanol. The purity and mass of each mutant were checked by electrophoresis and electrospray mass spectrometry.

Synthesis of Ligands. Dodecanoyl-CoA was synthesized and purified as previously described (11).

Isothermal Titration Calorimetry. Microcalorimetry was performed on a Microcal Omega titration microcalorimeter (Northampton, MA). Protein and ligand samples were prepared in 25 mM ammonium acetate (pH 6.0) and degassed under vacuum prior to analysis. Protein concentrations in

the sample cell (1.33 mL) were between 5 and 50 μM (typically 22 μM), and the temperature was 27 $^{\circ}\text{C}$. Ligand concentrations in the injection syringe (100 μL) were approximately 20 times higher than the corresponding protein concentrations. In a typical experiment, 25 aliquots of 4 μL of ligand were injected into a stirred (400 rpm) protein solution for a duration of 16 s with 2.5 min between injections. Data collection was achieved using the DSCITC software (MicroCal Inc.). Data evaluation, integration, analysis, and determination of binding parameters were performed using the Origin scientific plotting software (MicroCal Inc.) and the Calreg software (version 3.0), and isotherms were analyzed as described previously (16, 18). All experiments were repeated two to four times.

Equilibrium Denaturation. Solutions of GuHCl and 0.02 M sodium acetate (pH 5.3) were prepared at increments of 0.1 or 0.2 M GuHCl from a 6 M stock solution. The final concentrations were checked by refractive index. The intrinsic fluorescence at 356 nm was measured on a Perkin-Elmer LS50B apparatus from an excitation wavelength at 280 nm and slit widths of 5 nm; the protein concentration was 1 μ M. The fluorescence emission intensity of the protein solutions was followed until a stable signal was reached. All measurements were performed at 278 K. The temperature within the cuvette was checked manually using a thermocouple. The change in fluorescence intensity at 356 nm, f_{obs} , with concentration of denaturant was fitted to the following equation where f_N and f_D are the fluorescence of the native and denatured state, respectively, in the absence of denaturant:

$$f_{\text{obs}} = \{ (f_{\text{N}} + a_1[\text{GuHCl}]) + (f_{\text{D}} + a_2[\text{GuHCl}]) \exp([m([\text{GuHCl}] - [\text{GuHCl}]_{50\%}))/RT] \} / \{ 1 + \exp([m([\text{GuHCl}] - [\text{GuHCl}]_{50\%}))/RT] \}$$

where m is the slope of the transition and $[\text{GuHCl}]_{50\%}$ the concentration of denaturant at the midpoint of the transition. The effect of denaturant on the native and unfolded states was accounted for in the applied fit, where a_1 and a_2 are the linear dependence of denaturant concentration on the native and denatured states, respectively. R is the gas constant. The difference in free energy between the native and the denatured state, $\Delta G_{\text{D-N}}$, was calculated from the midpoint of transition, where $K_{\text{eq}}([\text{GuHCl}]_{50\%}) = 1$, as $\Delta G_{\text{D-N}} = m[\text{GuHCl}]_{50\%}$. All experiments were repeated at least two times.

Table 1: Thermodynamic Parameters for Stability and Ligand Binding of ACBP and Mutants

| mutant | ΔG_{D-N} (kcal mol ⁻¹) | ΔG_{bind} (kcal mol ⁻¹) | ΔH_{bind} (kcal mol ⁻¹) | $-T\Delta S_{bind}$ (kcal mol ⁻¹) | $\ln K_d$ (μ M) | SASA _{apo} ^a (Å ²) | SASA _{holo} ^b (Å ²) | ligand interaction ^c | vdW ^d |
|-------------------|---|--|--|--|----------------------|---|--|------------------------------------|------------------------------|
| WT | 7.89 ± 0.15 | -11.25 ± 0.27 | -7.43 ± 0.11 | -3.93 ± 0.34 | -5.60 ± 0.32 | — | — | — | — |
| F5A | 5.37 ± 0.34 | -9.17 ± 0.31 | -6.63 ± 0.10 | -3.25 ± 0.13 | -1.56 ± 0.15 | 0 | 0.5 ± 0.5 | — | D6, Y31, T35, A34, M70, Y73 |
| A9G | 6.08 ± 0.08 | -10.90 ± 0.13 | -7.53 ± 0.13 | -3.37 ± 0.18 | -4.42 ± 0.06 | 5.6 ± 4.1 | 7.5 ± 2.8 | Ade | Y31, Y73 |
| V12A | 6.20 ± 0.41 | -10.63 ± 0.16 | -7.16 ± 0.10 | -3.48 ± 0.19 | -4.02 ± 0.20 | 0 | 0 | — | L15, I27, V77, L80 |
| L15A | 4.79 ± 0.50 | -10.82 ± 0.15 | -11.48 ± 0.12 | -0.66 ± 0.19 | -4.34 ± 0.31 | 2 ± 2 | 0 | — | V12, P19, L80, Y84 |
| P19A | 6.82 ± 0.25 | -10.41 ± 0.08 | -5.66 ± 0.08 | -4.74 ± 0.11 | -3.47 ± 0.13 | 8.5 ± 4.2 | 0 | — | L15, M24, L80, Y84 |
| D21A ^e | 8.31 ± 0.47 | -11.9 ± 0.4 | -6.07 ± 0.01 | -5.8 ± 0.40 | -5.88 ± 0.54 | 41 ± 19 | 41 ± 11 | acyl | (K50, L25, K54) ^e |
| D21H ^e | 7.33 ± 0.11 | -10.4 ± 0.3 | -8.4 ± 0.1 | -2.0 ± 0.2 | -3.51 ± 0.23 | — | — | — | — |
| L25A | 6.87 ± 0.32 | -10.10 ± 0.13 | -6.47 ± 0.13 | -3.62 ± 0.18 | -2.92 ± 0.28 | 15 ± 5 | 40 ± 11 | acyl | A53, K54, A57 |
| Y28A | 5.42 ± 0.37 | -8.91 ± 0.16 | -4.57 ± 0.14 | -4.34 ± 0.22 | -1.11 ± 0.28 | 39 ± 7 | 2 ± 2 | Ade | K32, K54, W58 |
| Y28F | 6.83 ± 0.55 | -8.7 ± 0.4 | -6.64 ± 0.07 | -2.1 ± 0.3 | -0.60 ± 0.58 | — | — | — | — |
| Y28N | 5.66 ± 0.52 | -8.47 ± 0.03 | -5.0 ± 0.4 | -3.5 ± 0.5 | -0.37 ± 0.04 | — | — | Ade | — |
| Y31N ^e | 6.37 ± 0.59 | -9.1 ± 0.4 | -3.8 ± 0.5 | -5.3 ± 0.9 | -1.27 ± 0.61 | 52 ± 7 | 31 ± 2 | Ade | F5, A9, K32, T35, Y73 |
| K32A | 6.87 ± 0.73 | -7.98 ± 0.02 | -6.90 ± 0.30 | -1.10 ± 0.3 | 0.43 ± 0.03 | 42 ± 5 | 11 ± 4 | Ade | Y28, Y31, W58 |
| K32R | 6.06 ± 0.79 | -9.51 ± 0.04 | -6.8 ± 0.2 | -2.7 ± 0.2 | -2.12 ± 0.08 | — | — | Ade | — |
| K32E | 6.21 ± 0.48 | -7.83 ± 0.07 | -8.9 ± 0.4 | 1.1 ± 0.3 | -0.69 ± 0.12 | — | — | — | — |
| Q33A | 4.23 ± 0.34 | -10.79 ± 0.12 | -10.34 ± 0.11 | -0.42 ± 0.16 | -4.14 ± 0.19 | 0 | 0 | — | W58, L61 |
| A34G | 6.32 ± 0.24 | -11.38 ± 0.25 | -6.86 ± 0.10 | -4.52 ± 0.28 | -4.96 ± 0.28 | 0 | 0 | — | F5, T35, A69, M70 |
| T35A | 6.80 ± 0.35 | -10.8 ± 0.2 | -6.5 ± 0.2 | -4.30 ± 0.4 | -4.14 ± 0.31 | 13 ± 1 | 16 ± 2 | — | F5, Y31, A34, V36 |
| P44A | 6.49 ± 0.31 | -10.86 ± 0.22 | -7.39 ± 0.12 | -3.47 ± 0.26 | -4.34 ± 0.31 | 31 ± 11 | 33 ± 12 | — | R43, G45, D48, G51, K52, W55 |
| K52M ^e | 8.07 ± 0.46 | -10.08 ± 0.06 | -10.1 ± 1.1 | 0.05 ± 1.07 | -3.08 ± 0.65 | 57 ± 21 | 47 ± 17 | — | R43, P44, D48, F49, A53 |
| K54A | 7.03 ± 0.55 | -9.46 ± 0.11 | -7.82 ± 0.16 | -1.64 ± 0.19 | -2.00 ± 0.20 | 53 ± 10 | 9 ± 7 | Ade | — |
| K54M | 8.16 ± 0.52 | -9.85 ± 0.08 | -9.7 ± 0.1 | -0.11 ± 0.03 | -2.69 ± 0.15 | — | — | Ade | — |
| E67A | 7.53 ± 0.90 | -11.03 ± 0.27 | -6.94 ± 0.11 | -4.09 ± 0.29 | -4.51 ± 0.36 | 85 ± 19 | 81 ± 17 | — | K66, K71, S1, S65 |
| Y73A | 3.06 ± 0.27 | -9.12 ± 0.05 | -7.82 ± 0.19 | -1.30 ± 0.19 | -1.35 ± 0.08 | 1.4 ± 1.2 | 0 | Ade | F5, A8, A9, I27, H30, Y31 |
| Y73F | 8.16 ± 0.52 | -9.56 ± 0.06 | -6.8 ± 0.3 | -2.8 ± 0.3 | -2.25 ± 0.06 | — | — | Ade | — |
| V77A | 6.75 ± 0.23 | -10.56 ± 0.16 | -5.59 ± 0.24 | -4.98 ± 0.29 | -3.82 ± 0.08 | 0 | 0 | — | A8, V12, I27, L80 |
| L80A | 4.19 ± 0.20 | -10.78 ± 0.09 | -7.85 ± 0.17 | -2.93 ± 0.19 | -4.27 ± 0.14 | 3.2 ± 2.4 | 0 | — | V12, L15, Q33, I27, Y84 |
| K52M/ K54M | 8.90 ± 0.90 | -9.65 ± 0.11 | -10.5 ± 0.2 | 0.90 ± 0.06 | -2.35 ± 0.06 | — | — | Ade | — |

^a SASA_{apo} is the solvent accessible surface area calculated for apo-ACBP (2abd) using the program NACCESS (20). ^b SASA_{holo} is the solvent accessible surface area calculated for holo-ACBP (1aca) using the program NACCESS (20). ^c Ligand interactions calculated using the program XPLORE 3.0 (21) for holo-ACBP (1aca). Ade is the adenosine 3'-phosphate group, and acyl is an acyl chain. ^d Consistent van der Waals contacts between side chains in apo-ACBP (2abd) calculated using the program X-PLOR 3.0 (20). ^e Nonconserved residue.

Kinetic Refolding and Unfolding. Proteins were dissolved to concentrations between 0.33 and 1.0 mg/mL. Refolding and unfolding kinetics were measured as described previously (5).

RESULTS

Design Strategy. The contribution of each of the conserved residues in the ACBP family to the structure, function, and stability was analyzed using single-site mutations (Figure 2). The choice of mutations was as a first approach restricted to alanine substitutions at the majority of the conserved positions of the ACBP family. As ACBP is a predominantly α -helical protein, and since alanine is the least helix-opposing residue (19), these mutations were anticipated not to interfere with the geometrical parameters of the structural scaffold. Additionally, charge reversals or neutralizations of charges were applied on a subset of the residues. These substitutions were based on the knowledge of possible interactions between the ligand and ACBP as judged from large perturbations in chemical shifts in the NMR spectra of the complex. These residues are Tyr28, Tyr31, Lys32, Thr35, and Lys54. Furthermore, Asp21 was also chosen for substitutions since in the free protein, this side chain is suggested to participate in a bifurcated salt bridge to Lys50 and Lys54 (14, 15), an interaction that is missing in the complex (13). Some conserved sequence positions were not mutated; these were the two tryptophans (Trp55 and Trp58), the three glycines (Gly37, Gly45, and Gly67), and Ala69, Val36, and Ser65.

The expression and purification of all mutant proteins were successful, and all proteins were stable and existed in a native folded form at room temperature. The purity of the preparations was checked by mass spectrometry and N-terminal sequencing and was in all cases better than 98%.

Protein Stability. The difference in free energy between the denatured and the native state, ΔG_{D-N} , was measured for each mutant with guanidinium chloride titrations. The stability of the mutant proteins varied from a ΔG_{D-N} of 3.03 kcal mol⁻¹ (Y73A) to a ΔG_{D-N} of 8.90 kcal mol⁻¹ (K52M/K54M) (Table 1). For all the mutant proteins, the reversibility of the folding and unfolding processes was demonstrated by comparison of the refolding and folding kinetics to the equilibrium folding results (6). Most mutant proteins were destabilized ($\Delta\Delta G_{D-N(wt-mut)} > 0$) compared to the wild type bovine protein with the destabilizing effect introduced by the mutations [$\Delta\Delta G_{D-N(wt-mut)}$] being typically within 1–2 kcal mol⁻¹. A few mutations did stabilize the protein significantly [$\Delta\Delta G_{D-N(wt-mut)} < 0$], although the effects were small. These mutations are D21A and the double mutant K52M/K54M. A group of mutations showed a large and significant effect on the stability [$\Delta\Delta G_{D-N(wt-mut)} > 1.5$ kcal mol⁻¹]. These mutations are F5A, A9G, V12A, L15A, Y28A, Y28N, K32A, K32R, Q33A, A34G, Y73A, V77A, and L80A. The change in stability observed for the Y28F and Y73F mutants was marginal, whereas the change in stability of the Y28A, Y28N, and in particular Y73A mutants was highly significant. This suggests that only the aromatic

groups and not the hydroxyls play a role in providing stability to the ACBP proteins.

Binding Affinity and Energy. Binding of the ligand dodecanoyl-CoA to ACBP and its variants is mostly enthalpically driven, but with favorable entropy contributions (12). In this study, the ligand dodecanoyl-CoA was used which is shorter by four methylene groups than the ligand hexadecanoyl-CoA used in determining the NMR structure of the complex. This of course has an influence on probing residues which are important for acyl binding as the binding affinity is known to increase dramatically for longer acyl chains (11). Most likely, the residues important for acyl affinity will not be probed by the ligand dodecanoyl-CoA. The reason for choosing the dodecanoyl-CoA as a ligand in these studies is that hexadecanoyl-CoA binds to ACBP with a much higher affinity ($K_d \approx 10$ nM). Unfortunately, this is outside the window of accurate measurements with ITC.

All mutant proteins were able to bind the ligand with a high affinity, and the thermodynamic parameters could be measured readily (Table 1 and Figure 3). Typically, the binding affinity was decreased as a result of mutation (Figure 4). The most severe changes were observed for K32A [$\Delta \ln K_{d(wt-mut)} = -6.03$] and K32E [$\Delta \ln K_{d(wt-mut)} = -4.91$]. The free energy of binding dodecanoyl-CoA (ΔG_{bind}) varied from -11.9 ± 0.4 (D21A) to -7.83 ± 0.07 kcal mol $^{-1}$ (K32E) (Table 1). The change in binding energy [$\Delta \Delta G_{bind(wt-mut)}$] as a result of a mutation was most pronounced for mutations involving neutralization of charges or charge reversals. Also, one of the nonpolar residues which were truncated, F5A, showed a large decrease in binding energy. The largest effects [$\Delta \Delta G_{bind(wt-mut)} < -1.5$ kcal mol $^{-1}$, and $\Delta \ln K_{d(wt-mut)} < -2.5$] were observed for mutations F5A, L25A, Y28A, Y28F, Y28N, Y31N, K32R, K52M, K54A, Y73A, Y73F, and K52M/K54M (Figure 4).

Enthalpy and Entropy of Ligand Binding. The changes in the parameters of enthalpy (ΔH_{bind}) and entropy (ΔS_{bind}) contributing to ligand binding energy were typically larger than the change in ΔG_{bind} (Table 1). These changes divided the mutant proteins into three groups (Figure 5 and Table 2). The first group consists of mutations that result in no apparent change in either the binding energy or the enthalpy or the entropy contributions. These mutations concern A9G, V12A, L25A, A34G, T35A, P44A, E67A, and L80A. The second group of mutations shows no or little change in the binding affinity and energy, but large compensatory changes in enthalpy and entropy [$\Delta \Delta G_{bind} < 1.5$ kcal mol $^{-1}$, $|\Delta \Delta H_{bind}| \approx |\Delta(-T\Delta S)_{bind}|$]. These compensatory changes were seen as more favorable enthalpy combined with less favorable entropy (L15A, D21H, Q33A, and K52M) or as less favorable enthalpy combined with more favorable entropy (P19A, D21A, and V77A). The third and last group consists of mutations that caused a large change in binding energy ($\Delta \Delta G_{bind} < 1.5$ kcal mol $^{-1}$) but with noncompensatory changes in enthalpy and entropy. Again, there is a subdivision of the mutations. Either both the enthalpy and the entropy contributions were less favorable compared to those of the wild type (F5A, Y28F, Y28N, K32A, K32R, and Y73F), or they changed opposite (Y28A and Y31N, less favorable enthalpy and more favorable entropy; K32E, K54A, K54M, Y73A, and K52M/K54M, more favorable enthalpy and less favorable entropy). The grouping of

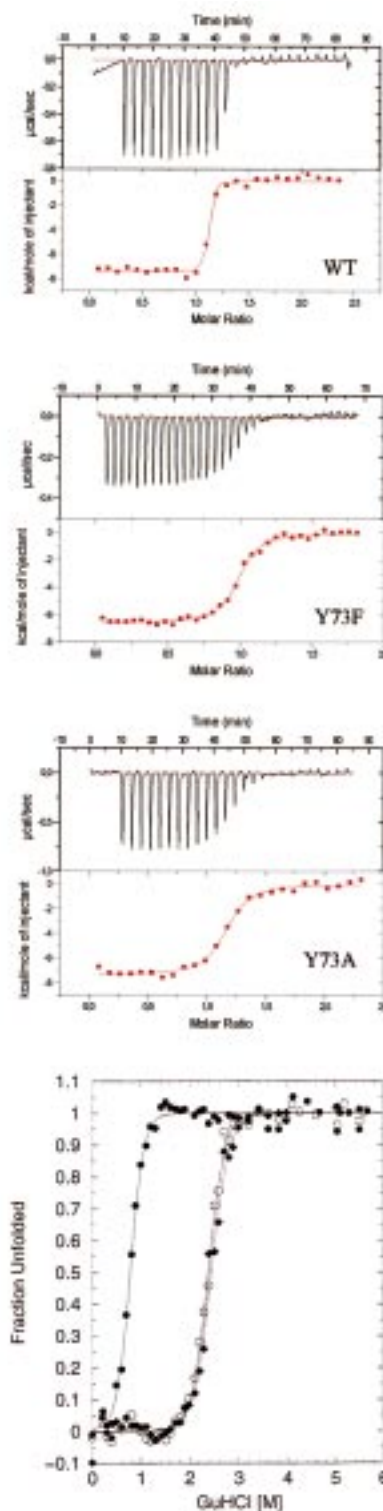


FIGURE 3: Isothermal titration and equilibrium denaturation of wild type bovine ACBP and Y73A and Y73F mutants. (A, top three panels) Binding isotherms for the titration of wild type bovine ACBP, Y73F, and Y73A with dodecanoyl-CoA. A 20 μ M solution of ACBP was titrated with 25 aliquots of 4 μ L injections of 0.5 mM dodecanoyl-CoA. The area under each injection was integrated and plotted in the bottom panel of each of the figures. The solid lines represent a nonlinear least-squares fit of the heat of each injection with the assumption of a single binding site. (B, bottom panel) The denaturation by GuHCl as described in the legend of Figure 3A: (●) Y73A and (○) wild type bovine ACBP and (◆) Y73F.

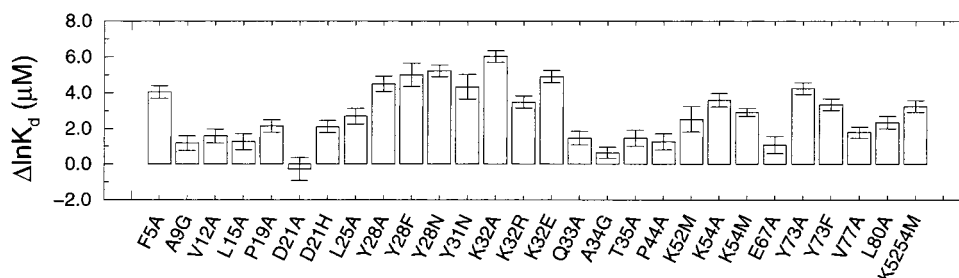


FIGURE 4: Relative changes in the dissociation constant for dodecanoyl-CoA. The changes in dissociation constant of the mutated variants are compared to those of wild type bovine ACBP [$\Delta \ln K_{d(wt-mut)}$].

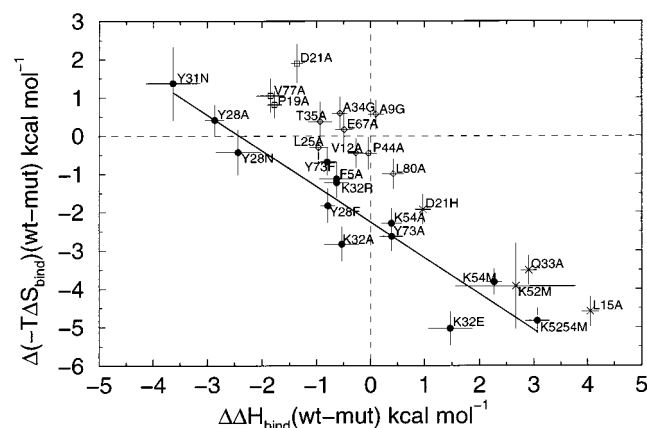


FIGURE 5: Correlation between the relative changes in enthalpy and in entropy by mutations. The mutations are shown as four individual groups with each of their marks. Binding site residues, where mutations cause large changes in binding energy ($\Delta \Delta G_{bind} > 1.5 \text{ kcal mol}^{-1}$), are shown as black circles, and a linear regression of these data gives a correlation coefficient R of 0.94 (solid line). Mutations of residues causing no effect on binding are shown as white diamonds, and mutations of residues resulting in compensatory changes in enthalpy and entropy and no large effect on binding energy are shown as white squares (hydrophobic changes) and stars (polar changes). For grouping of mutant proteins, refer to Table 2. Dotted lines indicating no change are drawn to guide the eye.

mutations according to these changes in binding energy, enthalpy, and entropy is listed in Table 2.

DISCUSSION

Conserved Residues and Their Role in Bovine ACBP. The mutations introduced in the sequence of bovine ACBP result in changes of both the thermodynamics of ligand binding and protein stability. The relative changes observed in protein stability, the binding affinity and energy, and in the contributing parameters of enthalpy and entropy divide the mutations into distinct groups (Table 2). From the changes observed as a result of the mutations, it is recognized that some mutations affect one of the parameters more than others and that one conserved residue may be important in fulfilling more than one distinct role. In the following, the mutated sites are described structurally and the effects of mutation on binding and stability are analyzed within this context. For this purpose, the solvent accessible surface areas of the individual side chains (SASA) and consistent van der Waals contact (vdW) with other side chains have been calculated for both apo-ACBP and holo-ACBP and listed in Table 1.

Conserved Residues and Protein Stability. The difference in free energy between the folded, native ACBP structure, which is capable of ligand binding, and the denatured,

unfolded peptide chain is only marginal, and the residues contributing to favorable interactions are therefore highly important. In a set of homologous protein sequences, the fundamental residues that provide this favorable interaction energy may be identified among the set of conserved sequence positions. For the mutations introduced in the bovine ACBP sequence which to a large extent cover the conserved sequence sites, only a subset of the mutations showed a large and significant effect on the stability [$\Delta \Delta G_{D-N(wt-mut)} > 1.5 \text{ kcal mol}^{-1}$]. The sequence sites involved are Phe5, Ala9, Val12, Leu15, Tyr28, Lys32, Gln33, Ala34, Tyr73, Val77, and Leu80. The positions of these residues are highlighted in the structure of bovine ACBP (Figure 6).

In the structures of ACBP, the conserved residues for which mutations cause a large destabilization effect are highly interconnected. These residues are localized at helix-helix interfaces, forming a pronounced hydrophobic interaction network between helix A1, helix A2, and helix A4 and between helix A2 and helix A3. Strong interactions are seen between Phe5, Ala9, Ala34, and Tyr73 and between Val12, Leu15, Val77, and Leu80. Likewise, strong interactions are seen between Tyr28, Lys32, and Gln33. For Tyr28, there are vdW interactions with Lys32, Lys54, and Trp58. Lys32 and Lys54 have been mutated in such a way that the effect of removing the entire hydrophobic side chain can be evaluated. However, only K32A and not K54A destabilized the structure significantly. It is possible that mutations of Trp58 may destabilize ACBP to the same extent as the mutations introduced at Tyr28. This residue is seen in Figure 7, and its position suggests that it may indeed constitute one of the helix-helix interface residues between helix A2 and helix A3 together with Tyr28, Lys32, and Gln33. Attempts to produce the W58A mutant protein have been unsuccessful, so milder mutations to a phenylalanine may be needed to confirm its involvement in providing stability at the interface between helix A2 and helix A3.

It is also interesting that all the sites for which mutations cause a large decrease in stability are all conserved. None of the mutations performed at nonconserved positions, D21A, D21H, Y31N, and K52M, showed a large destabilizing effect. More interesting, the conserved residues providing structural stability to ACBP are mostly hydrophobic. For Lys32, only removal of the large hydrophobic part of its side chain results in a destabilization of the protein; not even charge reversal (i.e., K32E) destabilized ACBP significantly. Only one polar residue, Gln33, is important for stability. Its polar side chain is completely inaccessible to solvent, and it is involved in an intense network of complex hydrogen bonds, which compensates for this unfavorable burial (Figure 7). It forms

Table 2: Grouping of Bovine ACBP Mutant Proteins According to Effects on Ligand Binding Energy, Enthalpy, and Entropy

| effect | no effects on binding | compensatory changes | large effects on binding |
|--------------------------------------|--|---|--|
| limits | $\Delta\Delta G_{\text{bind}} < 1.5 \text{ kcal mol}^{-1}$ $\Delta\Delta H_{\text{bind}} < 1 \text{ kcal mol}^{-1}$ $\Delta(-T\Delta S_{\text{bind}}) < 1 \text{ kcal mol}^{-1}$ | $\Delta\Delta G_{\text{bind}} < 1.5 \text{ kcal mol}^{-1}$ $ \Delta\Delta H_{\text{bind}} \approx \Delta(-T\Delta S_{\text{bind}}) $ | $\Delta\Delta G_{\text{bind}} > 1.5 \text{ kcal mol}^{-1}$ $\Delta\Delta H_{\text{bind}} > 1 \text{ kcal mol}^{-1}$ $\Delta(-T\Delta S_{\text{bind}}) > 1 \text{ kcal mol}^{-1}$ |
| $\Delta\Delta H_{\text{bind}}^a$ | — | ↑ | ↓ |
| $\Delta(-T\Delta S_{\text{bind}})^a$ | — | ↓ | ↑ |
| mutant | A9G V12A L25A A34G T35A P44A E67A L80A | L15A D21H Q33A K52M | P19A D21A V77A F5A Y28F Y28N K32A K32R Y73F Y28A Y31N K54A K54M Y73A K52M+K54M |

^a (↑) Increased effect of mutation; (↓) decreased effect of mutation.



FIGURE 6: Mapping stability to the structure of apo-ACBP. The conserved residues for which mutations affect protein stability significantly [$\Delta\Delta G_{\text{D-N(wt-mut)}} > 1.5 \text{ kcal mol}^{-1}$] are shown as gray space filling atoms and labeled with their residue number. Their position at the interfaces between the four helices is clear. The four helices are shown as solid rods, and a smooth ribbon drawn through the protein backbone atoms is shown in light gray. Trp58 is shown in black lines.

hydrogen bonds with the main chain amide of Thr64, with the main chain carbonyl of Gly37, and with the side chain of Asp38.

Conserved Residues and Ligand Binding Affinity and Energy. In this study, the ligand dodecanoyl-CoA (C_{12} -CoA) was used to probe the binding profile of bovine ACBP and 28 mutant proteins. From the structure of the complex between bovine ACBP and hexadecanoyl-CoA (C_{16} -CoA), it is evident that four methylene groups in the ω -end of the chain are making specific hydrophobic interactions with the protein. The affinity for the ligand dodecanoyl-CoA (C_{12} -CoA) resides therefore mostly in the electrostatic interactions between the CoA head and ACBP, especially with the 3'-phosphate group which has been shown to be responsible for around 40% of the binding energy (12). The affinity for the acyl chain, which resides mostly in the ω -end, is not probed by this ligand.

Seven residues for which mutations affected ligand binding affinity and energy dramatically have been identified. These residues are Phe5, Leu25, Tyr28, Tyr31, Lys32, Lys54, and Tyr73. Six of these seven residues are involved directly in

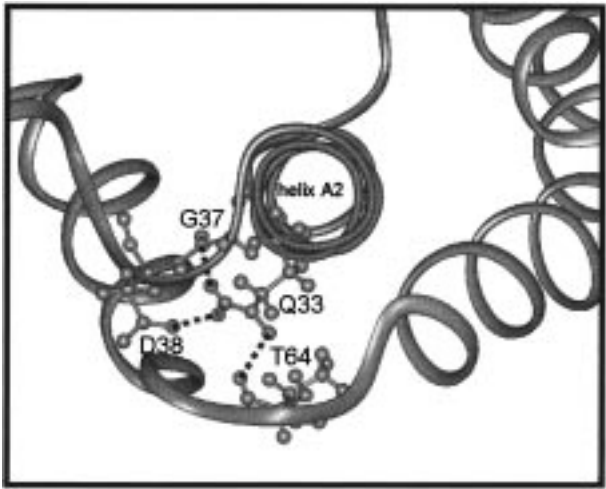


FIGURE 7: Local environment of Gln33 in the structure of bovine ACBP. The massive network of hydrogen bonds is clearly visible.

binding of the adenosine 3'-phosphate part of the CoA, and can be seen in Figure 1, where they are highlighted in the structure of the complex of bovine ACBP and hexadecanoyl-CoA. Direct interactions are clearly present between 3'-phosphate and the adenine ring and residues Tyr28, Tyr31, Lys32, Lys54, and Tyr73. Phe5 is not making direct interactions with the CoA head. For Phe5, there are large interaction areas to especially two residues, Tyr31 and Tyr73. The decreased binding affinity and energy for the F5A mutant may result from a structural rearrangement of Tyr31 and Tyr73 as removal of the phenyl group of Phe5 most likely collapses the aromatic lock formed by these three residues and thus weakens the interactions with the adenine ring. Leu25 is interacting with residues Ala53, Lys54, and Ala57, forming interactions with the ω -end of the ligand. It is shielded from solvent in apo-ACBP by Glu22, and in the complex Glu22 changes its position, such that the solvent accessibility of the side chain of Leu25 changes from 15 to 40%. Leu25 can be viewed as the bottom of the hydrophobic cave between helix A2 and helix A3, stabilizing the hydrophobic cleft. The mutation of the side chain to an alanine seems to have a long-range effect that propagates to affect also binding of a medium-length acyl-CoA such as dodecanoyl-CoA. It may be anticipated that the change observed in binding affinity for the L25A mutant protein would be even larger when hexadecanoyl-CoA is the ligand. All the residues for which mutations cause a decrease in

binding affinity and energy are highly conserved in the set of homologous ACBPs, and many of these contain both a polar functional group and a large hydrophobic part. Tyr31 is not strictly conserved but is found only as a tyrosine or phenylalanine which represents a conservative change that still enables the aromatic stacking with the adenine ring of the CoA head. It is interesting to notice that the changes in binding affinity and energy for mutations involving Tyr28 and Tyr73 are confined to the removal of the hydroxyl groups, suggesting that the aromatic and hydrophobic interactions are not important for ligand binding but more so for protein stability.

Conserved Residues and Ligand Binding Enthalpy and Entropy. The free energy for binding of dodecanoyl-CoA to wild type bovine ACBP is -11.25 ± 0.27 kcal mol⁻¹ (Table 1). This amount of energy results from the sum of contributions arising from stabilization of the protein in the holo form compared to the apo form, from the energy difference between the solvated and the bound ligand, and from energies for interaction between the ligand and ACBP. A difference in the binding energy between wild type ACBP and a mutant protein will reflect changes in any of these three energy origins. It is possible that the three individual terms will make opposite contributions, which in that case will lead to no change in binding energy. This, however, may seldom be the case.

The mutations introduced in the sequence of bovine ACBP which result in an effect on the thermodynamics of ligand binding can be grouped according to their changes in binding energy. One group of mutations comprises those with major changes in binding affinity and energy. This group of seven residues has already been described. The individual effects on the enthalpy and entropy of binding on the other hand reflect the type of interactions that are important for ligand binding and which have been abolished by the mutation. For these seven residues, there are different dominating effects dependent on the degree of mutations. For F5A, Y28F, Y28N, K32A, K32R, and Y73F, there is a concomitant change in both enthalpy and entropy, suggesting that both polar and hydrophobic interactions are lost by the mutations. For Y28A and Y31N, there are an increase in enthalpy and a decrease in entropy, showing that the loss of hydrophobic interactions is dominant, whereas for K32E, K54A, K54M, Y73A, and K52M/K54M, the opposite is the case and loss of polar interactions dominates. These conclusions are in accordance with the structural arrangement of the ligand and the participating binding residues (Figure 1). The loss of electrostatic interactions with the 3'-phosphate may result in loosening of the hydrophobic interactions between on one hand the adenine ring and the aromatic rings of ACBP and on the other hand between the aromatic rings of ACBP themselves. Using the same arguments, it is also clear that Lys54 does not contribute with any significant hydrophobic interaction to ligand binding.

Another group of mutations consists of those for which compensatory changes in enthalpy and entropy result in little or no change in binding energy. These changes reflect changes in the protein structure, which again result from compensatory changes arising from structural rearrangements or from removal of important protein-protein interactions. Pro19 and Val77 are interacting with the residues at the

interface between helix A1 and helix A4, and truncation of these two residues does not affect binding energy. Rather, the mutations destabilize the protein, both in the apo and in the holo forms. The side chain of Lys52 is hydrogen bonded to backbone carbonyls of either Met46 or Pro44, and the removal of this interaction is reflected in the increase in enthalpy and decrease in entropy. The side chain of Gln33 is completely buried and hydrogen bonded and its interaction network described under the subsection of protein stability. Asp21 is not a conserved residue, and is seen as Asp, Asn, and Thr. It forms specific interactions with the ω -end of the ligand, which for dodecanoyl-CoA may be less interesting. Substitutions with Ala and with His have opposite effects on the enthalpy and entropy. This suggests that compared to wild type bovine ACBP, more hydrophobic surface is exposed in the D21A mutant protein and more polar surface is exposed in the D21H mutant protein. Mutation L15A is interesting in that removal of the leucine side chain, which has strong interactions at the helix-helix interface between the N- and C-terminal helices, would be expected to result in loss of hydrophobic interaction. Instead, the changes in enthalpy and entropy observed point to a loss of more polar than nonpolar interactions. One explanation may be a destabilization of the helix-helix interface, preventing formation of a double salt bridge between side chains of Lys76, Lys81, and Glu11.

Conservation of Residues in Homologous Proteins. In the family of 24 highly homologous ACBP sequences, there are 26 sequence sites which have been conserved throughout evolution of the eukaryotic kingdoms. These sites include both polar and nonpolar residues and are spread throughout the sequence with a contiguous stretch of six residues from Lys32 to Gly37. The evolutionary pressure exerted on the structure, function, stability, and folding ability of the ACBP family of proteins has involved an interconnected optimization process in which each conserved residue may play a specific role. The roles of the conserved sites have been probed by single-site mutations. Initially, the role of the conserved residues for an efficient protein folding reaction was established in an earlier study (6). Eight hydrophobic conserved residues, Phe5, Ala9, Val12, Leu15, Tyr73, Ile74, Val77, and Leu80, form the interaction interface between N- and C-terminal helices A1 and A4 in the folding rate-limiting structure. In this study, it is found that typically, loss of binding affinity and energy is only associated with a small change in stability, whereas a large change in stability is only associated with a small change in binding energy. For a few residues, mutations could introduce a large change in both parameters, but in these cases, removal of a shorter piece of the side chain alone would cause the change in binding energy. Therefore, conserved residues in the ACBP family may have been evolutionally conserved for fulfilling more than one role. Tyr73 is one such example. The results also indicate that conservation of residues in homologous proteins may result from optimization of a set of parameters, which is an effective folding reaction, a stable native protein, and a fully active binding site. This is important in protein design strategies, where optimization of one of these physical parameters, typically function or stability, may influence any of the others markedly.

ACKNOWLEDGMENT

We thank Jens S. Andersen for help with the mass spectrometric analysis and Jens Roswalld Andersen, Erling Knudsen, and Pia Skovgaard for skilled technical assistance.

REFERENCES

1. Færgeman, N. J., and Knudsen, J. (1997) *Biochem. J.* 323, 1–12.
2. Rischel, C., Andersen, K. V., Madsen, J. C., and Poulsen, F. M. (1994) *Biochemistry* 33, 13997–14002.
3. Kragelund, B. B., Robinson, C. V., Knudsen, J., Dobson, C. M., and Poulsen, F. M. (1995) *Biochemistry* 34, 7217–7224.
4. Kragelund, B. B., Knudsen, J., and Poulsen, F. M. (1995) *J. Mol. Biol.* 250, 695–705.
5. Kragelund, B. B., Højrup, P., Jensen, M. S., Schjerling, C. K., Juul, E., Knudsen, J., and Poulsen, F. M. (1996) *J. Mol. Biol.* 256, 187–200.
6. Kragelund, B. B., Osmark, P., Neergaard, T. B., Schiødt, J., Kristiansen, K., Knudsen, J., and Poulsen, F. M. (1999) *Nat. Struct. Biol.* (In press).
7. Eriksson, A. E., Baase, W. A., Wozniak, J. A., and Matthews, B. W. (1992) *Nature* 355, 371–373.
8. Morton, A., and Matthews, B. W. (1995) *Biochemistry* 34, 8576–8588.
9. Richieri, G. V., Low, P. J., Ogata, R. T., and Kleinfeld, A. M. (1997) *J. Biol. Chem.* 272, 16737–16740.
10. Richieri, G. V., Low, P. J., Ogata, R. T., and Kleinfeld, A. M. (1998) *J. Biol. Chem.* 273, 7397–7405.
11. Rosendal, J., Ertbjerg, P., and Knudsen, J. (1993) *Biochem. J.* 290, 321–326.
12. Færgeman, N. J., Sigurskjold, B. W., Kragelund, B. B., Andersen, K. V., and Knudsen, J. (1996) *Biochemistry* 35, 14118–14126.
13. Kragelund, B. B., Andersen, K. V., Madsen, J. C., Knudsen, J., and Poulsen, F. M. (1993) *J. Mol. Biol.* 230, 1260–1277.
14. Andersen, K. V., and Poulsen, F. M. (1993) *J. Mol. Biol.* 226, 1131–1141.
15. Andersen, K. V., and Poulsen, F. M. (1994) *J. Biomol. NMR* 3, 271–284.
16. Wiseman, T., Williston, S., Brandts, J. F., and Lin, L. N. (1989) *Anal. Biochem.* 17, 131–137.
17. Mandrup, S., Hummel, R., Ravn, S., Jensen, G., Andreasen, P. H., Gregersen, N., Knudsen, J., and Kristiansen, K. (1991) *Biochem. J.* 276, 817–823.
18. Sigurskjold, B. W., Altman, E., and Bundle, D. R. (1991) *Eur. J. Biochem.* 197, 239–246.
19. O'Neil, K. T., and Degrado, W. F. (1990) *Science* 250, 646–651.
20. Hubbard, S. J., and Thornton, J. M. (1993) *NACCESS*, Department of Biochemistry and Molecular Biology, University College London, London.
21. Brünger, A. T. (1992) *The X-PLOR Software Manual*, version 3.0, Yale University Press, New Haven, CT. BI982427C